Global patterns for the spatial distribution of floating microfibers: Arctic Ocean as a potential accumulation zone

André R.A. Lima [a,*], Guilherme V.B. Ferreira [b], Abigail P.W. Barrows [c], Katie S. Christiansen [d], Gregg Treinish [d], Michelle C. Toshack [d]

[a] *Marine and Environmental Sciences Centre, ISPA – University Institute, Department of Biosciences, 1149-041, Lisbon, Portugal*
[b] *Federal Rural University of Pernambuco, Department of Fishing and Aquaculture, Recife, Brazil*
[c] *College of the Atlantic, Department of Biology, 105 Eden Street, Bar Harbor, ME, 04609, USA*
[d] *Adventure Scientists, PO Box 1834, Bozeman, MT, 59771, USA*

ABSTRACT

Despite their representativeness, most studies to date have underestimated the amount of microfibers (MFs) in the marine environment. Therefore, further research is still necessary to identify key processes governing MF distribution. Here, the interaction among surface water temperature, salinity, currents and winds explained the patterns of MF accumulation. The estimated density of floating MFs is $\sim 5900 \pm 6800$ items m^{-3} in the global ocean; and three patterns of accumulation were predicted by the proposed model: (i) intermediate densities in ocean gyres, Seas of Japan and of Okhotsk, Mediterranean and around the Antarctic Ocean; (ii) high densities in the Arctic Ocean; and (iii) point zones of highest densities inside the Arctic Seas. Coastal areas and upwelling systems have low accumulation potential. At the same time, zones of divergences between westerlies and trade winds, located above the tropical oceanic gyres, are predicted to accumulate MFs. In addition, it is likely that the warm branch of the thermohaline circulation has an important role in the transport of MFs towards the Arctic Ocean, emphasizing that surface water masses are important predictors. This study highlights that the Arctic Ocean is a dead end for floating MFs.

1. Introduction

Plastics have reached great proportions within the aquatic environments, estimated to be approximately 100 million tons within the ocean, positioning plastics pollution as one of the top environmental issues of the decade (Eriksen et al., 2014; Dauvergne, 2018; Herrera et al., 2020). Almost 90 % enter the sea from land-based sources (Lebreton et al., 2017). Over the last decade there has been a growing awareness of the general public towards plastic pollution, that put pressure on government agencies to implement regulatory actions (*e.g.* U.S. Microbead-Free Waters act of 2015 and European Commission, 2018). Therefore, during the 2019 Basel Conference in Geneva, Switzerland, ~180 governments identified plastics as hazardous wastes due to their toxicity, capacity of adsorbing pollutants and of fragmentation (Lima et al., 2020). The Basel Convention on the Control of Transboundary Movements of Hazardous Wastes and their Disposal is an international treaty aiming at reducing the movements of hazardous waste between nations (Niaounakis, 2017; Raubenheimer et al., 2018). In May 2019, after the joint meeting of three conference of the parties (Basel, Stockholm and Rotterdam conventions), where the trade of dangerous products among nations was discussed, it was concluded that to export hazardous waste from industrialized to least developed countries is illegal and the introduction of more effective amendments to better control international traffic and environmental impacts is necessary. What does this mean for certain classifications of plastics, namely synthetic and semi-synthetic fibers?

Within the plastic concept, the smaller particles (< 5 mm) known as microplastics (MPs) have gained more attention due to their potential to adsorb hazardous chemicals available in aquatic systems, such as metals and POPs, although their toxicity along the food web does not yet has been proved (Eriksen et al., 2018; Yu et al., 2019; Enfrin et al., 2020; Yang et al., 2020). MPs is acknowledged as ubiquitous in the marine environment as their diminutive size make them easily welcoming in biogeochemical and ecological processes (Remy et al., 2015; Zhao et al., 2016; Ferreira et al., 2019).

Microfibers (MFs) are even a special case thanks to their great availability in most marine samples (*e.g.* sediments, water and wildlife)

---

* Corresponding author.
  E-mail address: andre.ricardoaraujolima@gmail.com (A.R.A. Lima).

representing from 40 % to more than 90 % of the MP in most cases (Bergmann et al., 2017; Woodall et al., 2014; Barrows et al., 2018; Zhu et al., 2018; Ferreira et al., 2019). Despite this, there have been few efforts to discuss how the market of synthetic fabrics must behave in the current scenario of mitigation (Raubenheimer et al., 2018). The so-called source-to-sea continuum has been widely discussed to understand how the environmental gradient established among rivers, coasts and open ocean build the transboundary nature of MFs. Examples of MF sources are related to the release by washing machines and the use and maintenance of fishing nets, as observed worldwide, especially in underdeveloped countries (Wu et al., 2019; Li et al., 2020). This emphasizes that the widespread global pollution is connected by international impacts (Lima et al., 2014, 2020; Lebreton et al., 2017).

Synthetic fibers account for 60 % of the 9 million tons of fibers produced globally, polyester being the most common polymer produced in the global fiber market. Although up to 99 % of MPs, including MFs, can be removed from wastewater after conventional treatment (Gatidou et al., 2019), still nearly 2.5 million tons year^{-1} of this contaminant are transported from the continent to the ocean *via* river input (Boucher and Friot, 2017; Barrows et al., 2018; Mishra et al., 2019). This has proven that to date, the real quantity of MPs in the ocean had been underestimated by at least 3 orders of magnitude (Barrows et al., 2018; Conkle et al., 2018). Thus, such gap is relative to the underestimation of MFs in most studies using plankton nets (Barrows et al., 2018).

Therefore, new methodological procedures have been proposed to re-estimate the pollution of MPs and to assess whether the accumulation patterns proposed by previous models gave the complete picture of the fate of MPs in the global oceans (Amélineau et al., 2016; Sun et al., 2018; Mu et al., 2019). Particle tracking models with Lagrangian and Eulerian approaches have been widely used to simulate the trajectories of MPs according to the velocity fields from ocean general circulation models and have provided important conclusions regarding the fate of MPs in oceans under a global perspective (Lebreton et al., 2012; Maximenko et al., 2012; van Sebille et al., 2015v; Onink et al., 2019; Mountford and Morales Maqueda, 2019). Spatial correlative models might also aid information for the global distribution of MPs because they allow the inclusion of many other variables, such as salinity and water temperature to understand the influence of water masses; and near-surface winds, including insights on their influences in gyres and upwelling regions. However, this approach is still missing. In addition, it is acknowledged that to track the distribution of microplastics is difficult due to the disagreement between buoyancy capacity and the sinking nature of most particles (Hardesty et al., 2017; Cózar et al., 2017). Therefore, to couple predictions from different water masses and sediments along the entire ocean basin will be the only way to understand how floating MPs sink towards sediments and then come back to surface following major oceanic dynamics (Mountford and Morales Maqueda, 2019; Kane et al., 2020).

Correlative spatial modelling might be a powerful tool to track the pathways of MPs as ruled by the chemical and physical characteristics of water masses. Moreover, understanding distribution and accumulation patterns will provide information on predicted quantities in remote areas, regions with no source of pollution, and may even point out dead ends where MPs will peak in density. This will help managers and the scientific community to determine where to locate mitigation efforts. Therefore, we applied spatial modelling to predict the accumulation of floating MFs (< 1.5 mm–5 mm) using high-quality data collected by citizen scientists, that coupled with professional laboratory services, helped to estimate the density of floating microfibers in the global ocean. Citizen scientists are helping with large scale data collection leading to a better understanding of environmental issue somewhat difficult to assess due to expensive and time-consuming surveys (Barrows et al., 2018). This initiative raises awareness and engagement with environmental issues even outside of the scientific community (Zettler et al., 2017).

We hypothesize that floating MFs will have higher densities wherever the interactions of physical and chemical parameters provide suitable regions of accumulation. It is considered microfiber, every synthetic, semi-synthetic and non-synthetic material as revealed by µFT-IR. The principal objective of this study is to identify key oceanographic processes governing the fate of MFs based on field evidences and to produce global estimates for the distribution of floating MFs through GIS technique in the whole ocean surface. This study will orient future research and provide new information that, together with other models available to date, will help to better understand the distribution patterns of MFs.

2. Material and methods

2.1. Data collection

All the data used in this study was gathered by "one of the largest and most diverse global microplastic pollution datasets to date": the Adventure Scientists'Global Microplastics Initiative (https://www.adventurescientists.org/microplastics.html). Given the great extent of the study area and the lack of worldwide data bases regarding this pollutant, the public participation could be an important tool on development of scientific knowledge.

Citizen scientists followed the standards proposed by Barrows et al. (2017, 2018). Several measures were implemented to ensure accuracy and reliability of data. A total of 1393 Surface water samples were collected with 1 L bottles in rocky and sandy shorelines, offshore, estuaries, remote and urban locations (Fig. 1). During sampling, cautions such as triple rinsing with tap water, sealing and capping of samples underwater were used to reduce *in situ* airborne contamination.

At the laboratory, samples were vacuum filtered over a 0.45 µm filter and particles were counted under a stereomicroscope; or a compound microscope whenever a particle could not be confirmed as being MP under the stereomicroscope. Further precautions such as wiping down lab surfaces with cellulose sponge, triple rinsing of tools, glassware and petri dishes, wearing of 100 % cotton lab coats, and vacuuming of lab floor and surfaces were used to reduce airborne contamination. Additionally, to reduce the risk to overestimate MP, air and laboratory water blanks were run to assess contamination during sample handing, and procedural blanks were implemented during the identification of samples under the stereo microscope. At least 10 particles were randomly taken from 10 different samples belonging to each oceanic basin (n = 113 particles) to identify the particle material by micro Fourier Transform-Infrared Spectroscopy (µFT-IR) (Barrows et al., 2018). From these particles, the vast majority were classified as fibers 96 % (of which 69 % were identified as synthetic or semi-synthetic and 31 % as non-synthetic) and fragments represented only 4 % of particles (100 % synthetic). Blanks revealed MP contamination at 0.5 particles L^{-1} for lab water (n = 265) and 0.019 particles min^{-1} for air exposure (n = 126) from both synthetic and non-synthetic airborne contamination. Since contamination was not high, blank results were not subtracted from the field samples (Barrows et al., 2018).

2.2. Environmental data selection and manipulation of satellite layers

Satellite environmental data were used as explanatory variables to model the current distribution of MFs in the global oceans. At least 28 oceanographic variables among chemical and physical data were downloaded from respective databases (Table S1). Specifically, the mean, maximum, minimum and range of sea surface temperature (SST in °C), sea surface salinity (SSS in PSS) and current velocity (CVEL in m s^{-1}; determined with the Pythagoras theorem on the meridional and zonal components of ocean currents) (Assis et al., 2017); several data on northward/eastward wind and current components (*i.e.* velocities in m s^{-1}) (ESR, 2009; Dee et al., 2011; Mulet et al., 2012; Rascle and Ardhuin, 2013; Rio et al., 2014; Laurindo et al., 2017); wind speed at 10 m above the surface (WS in m s^{-1}) (Dee et al., 2011); sea surface density (SSD in kg m^{-3}) (Droghei et al., 2016); sea level anomaly (SLA in m) (Hijmans)
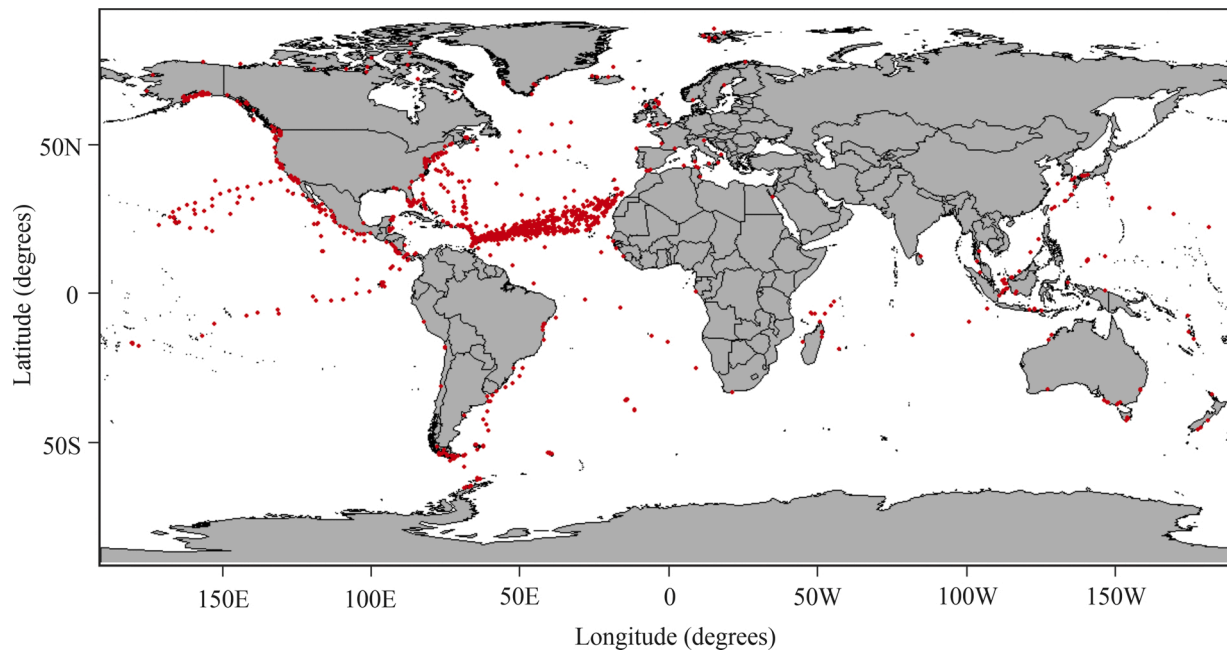
Fig. 1. Spatial points representing the locations of microplastic sampling. Geographic coordinate system: WGS 1984. R package: Maptools (https://cran.r-project.org/web/packages/maptools/index.html).

and number of drifter drogues (NDD in days per square degree) (Laurindo et al., 2017) were used. All these variables are considered important either as a direct influence on the MP distribution and accumulation or as proxies for causal factors. For example, the interaction between SST and SSS, as well as SSD, are a good proxy to differentiate water masses; the velocities and directions of winds and currents, as well as NDD (a proxy for buoyant data), can help to predict how MP will derive and accumulate; and the SLA, which varies with ocean processes such as gyres, meanders and eddies can help to predict whether MP is influenced by upwelling processes (negative SLA values) or downwelling processes (positive SLA values).

Every data are monthly-averaged satellite images from daily measurements processed and reanalysed as regular grids under a GIS (Geographic Information Systems) environment (Assis et al., 2017; Laurindo et al., 2017; Mertz and Legeais, 2019). A reanalysis is a scientific method for developing a comprehensive record of how weather and climate are changing over time and can help in the understanding of the present state of systems through synthesized global raster files (Table S1). The satellite variables were selected and downloaded according to their best resolution in order to obtain enough grid cells representing the environmental characteristics of each sampling point (Table S1). All predictors were statistically downscaled to a common spatial resolution of 0.083° (~9 arcmin) by fitting a kriging interpolation using the spatial analyst tools in ArcGis 10.4.1 (https://www.esri.com/) and the raster package (Hijmans et al., 2020) in R 3.6.2 (R Core Team, 2020).

2.3. Data analysis and spatial mapping

Before model runs, volume was converted from L to m^{-3} and atypical values were excluded whenever they were extremely different from the general observations within the same geographic region. The final dataset used in the model had the same proportion than the original matrix, being 91 % fibers and 9 % fragments. The final dataset has 6.855 MPs L^{-1} on average, being 6.208 MFs L^{-1} (or 6208 MFs m^{-3}) and 0.746069182 fragments L^{-1} (or 746 fragments m^{-3}) on average. The number of fragments were not included in the analysis, because it was not representative.

Generalized Additive Models (Hastie and Tibshirani, 1990) were

proposed to investigate the variability in the density of MFs (particles m^{-3}), the response variable (y_i) according to a set of continuous satellite environmental data, and the explanatory variables (x_i) [R 3.6.2 programming environment]. GAMs are more flexible simulation models widely used in spatial predictions because they do not use parametric (predefined) shapes, but rather let the data find the best solution to the shape by applying a selection of local smoothing functions (usually spline functions) along the gradients of explanatory variables, having superior performance relative to the polynomial functions used in linear models (Hastie and Tibshirani, 1990; Wood, 2006).

To analyse the behaviour of the response variable, initially MF data from 2013 to 2017 were pooled to represent the current distribution of MFs in the global oceans; and then, an exploratory data analysis to propose their distributions was performed. MFs are well fitted in a Tweedie distribution (Fig. S1), which is a special case of an exponential distribution, where a cluster of data items at zero (called a "point mass") followed by non-negative data points are observed (Tweedie, 1984). This family of distributions has a mean of $E(Y) = \mu$ and a variance of $Var(Y) = \varphi \mu^p$. The p in the variance function is an additional shape parameter for the distribution. "p" is sometimes written in terms of the shape parameter α: $p = (\alpha - 2) / (\alpha - 1)$ (Tweedie, 1984). Therefore, the Tweedie error distribution with the log link function was used for GAM fitting.

At least 300 GAMs were set a priori. To avoid the use of high correlated predictors in the same model, the correlation among layers was checked using a Pearson's correlation matrix. Only layers with correlation coefficient below 0.45 were included in the same model (Fig. S2). For each case, a model was built by testing all variables that were considered meaningful; and the best models were determined by fitting across the full set of possible models (See Table S2 and S3). The MGCV library in the R statistical software was used to select the GAM smoothing predictors (Wood, 2019). To help in the identification of important features, a double penalty was applied to the penalized regression of each model, allowing variables to be solved out of the model (Marra and Wood, 2011). The degree of smoothing was chosen based on the restricted maximum likelihood method (REML), which outperforms the generalized cross validation (GCV) smoothing parameter selection (Marra and Wood, 2011). To avoid overfitting, the number allowed to the smoothing functions were limited to 5 for single terms, 20

for two-interaction terms and 60 for three-interaction terms (Wood, 2006).

The goodness of fit of the models were checked by the lowest value of the Akaike's Information Criterion (AIC) (Hastie and Tibshirani, 1990) and the level of deviance explained (0–100 %; the higher the percentage, the more deviance explained). To validate the selected models, the normal probability QQ-plots of the residual components of the deviance *vs.* quantiles, as well as the observed *vs.* fitted values and residuals *vs.* linear predictors plots were evaluated to check model misspecification (Fig. S3). The output of the final selected GAM is presented as plots of the best-fitting smooths. Single and interaction effects are shown as perspective and 3-D plots, respectively. Based on validation results, the selected model was applied in a predictive mode to provide response estimates of MF distribution/accumulation over a wider grid of mean monthly satellite data at a GIS resolution of 0.083°, covering the entire ocean basins.

3. Results

3.1. Influences of physical and chemical variables in the accumulation of MFs

In total, 1272 samples, with an average density of 6208 ± 8133 MFs m^{-3}, collected from 2013 to 2017 were pooled to describe the current distribution of MFs in the global oceans. From the 300 GAMs set a priori, it was possible to select 20 GAMs to compare fitting performance (Table S2). It was possible to reduce the deviance from 5222.62–3302.60, increase the deviance explained from 6.3 % to 31 %, and reduce the AIC from 8737.58 to 6333,25. Therefore, the final GAM for pooled data included as main effects: WS and the interaction among SST, SSS and CVEL ($p < 0.001$) (Tables 1 and 2 and Fig. S4). All these parameters have Pearson's correlation values below 0.45 (Fig. S2 and Tables S3). The normal probability plots and the residuals from the full models are nearly normally distributed and the relationship between observed and fitted values had a positive correlation of 0.53, showing an adequate fit of the model (Fig. 4 and Fig. S2). In addition, the predicted average density of MFs extracted from the same georeferenced sampling area was 6243 MFs m^{-3}, which is similar to the average observed for the raw data (*i.e.* 6208 MFs m^{-3}).

The model predicted that the accumulation of MFs is more prone to respond to the role of surface water masses, as imposed by the interaction between SST and SSS. These water masses represent boundaries for the accumulation of MFs in specific oceanic regions. Thus, MFs will likely disperse following the general surface circulation patterns of water masses. MFs peak ($> 5 \times 10^4$ MFs m^{-3}) in areas where SST ranges between 6 and 8 °C and SSS between 30 and 32 PSS, a physico-chemical pattern observed towards the poles (Figs. 2, 3a and S4). Patterns of low accumulation are predicted in areas where SST ranges between 20 and 26 °C and SSS is above 20 PSS ($> 1 \times 10^4$ MFs m^{-3}). Regarding the interactions between CVEL *vs.* SSS *vs.* SST, it is predicted that the accumulation of MFs is intermediate ($> 1.2 \times 10^4$ MFs m^{-3}) in regions of slow CVEL (0.4 to 0.8 m s^{-2}), whenever SSS is above 36 PSS and SST is above 26 °C (Figs. 2 and 3b,c). Higher densities ($> 2.2 \times 10^4$ MFs m^{-3}) are predicted whenever CVEL is above 1 m s^{-2} and SSS is above 38 PSS, as observed towards the poles (Figs. 2, 3c and S4). Accumulation is not

Table 2
Selected GAM with goodness of fit statistics for microplastic density data (AIC: Akaike's information criterion, K: number of knots for smooth, Edf: estimated degrees of freedom). Model: MP ~ s(SST, SSS, CVEL) + s(WS).

Microplastic density (particles m^{-3})			
Coefficient	**Estimated ± S.E**		***P* value**
Intercept	1.99 ± 0.033		<2e-16 ***
	K	**Edf**	
s(SST, SSS, CVEL)	59	44.54	< 2e-16 ***
s(WS)	4	3.02	< 2e-16 ***
Deviance explained	31 %		
Null deviance	4066.11		
Deviance	3302.60		
Residual df	906.92		
AIC	6333.25		

predicted in regions where CVELs interact with SSS and SST below 20 PSS and 20 °C, respectively (Figs. 2 and 3b,c). Moreover, according to the single term, MFs are predicted to accumulate in regions where WS is between 5.5 and 8 m s^{-2}, a pattern observed mainly around the tropical gyres (Figs. 3d and S4).

3.2. Spatial mapping

The model predicted that the average global pollution with floating MFs is ~5900 ± 6800 MFs m^{-3}, ranging between 0 and ~113,000 MFs m^{-3} (Table 3). The highest average density of MFs was estimated in the Hudson Bay (~$27,000 \pm 18,000$ MFs m^{-3}), followed by the Arctic Seas (~$20,000 \pm 20,000$ MFs m^{-3}) and the Mediterranean (-~9000 ± 3000 MFs m^{-3}). The lowest densities were estimated in the small water bodies, such as the Red (~1770 ± 1190 MFs m^{-3}) and Black (~930 ± 460 MFs m^{-3}) seas, the Persian Gulf (~496 ± 630 MFs m^{-3}) and the Baltic Sea (~1760 ± 4500 MFs m^{-3}). Another region of low accumulation is estimated in the northern Atlantic (between 40 °N and 60 °N), where average density is ~1800 ± 1720 items m^{-3} (Table 3). Therefore, MFs exhibited three patterns of accumulation in global oceans: (i) intermediate densities in tropical and subpolar gyres, Seas of Japan and of Okhotsk, Mediterranean and around the Antarctic Ocean ($>5000 \pm 1440$ to ~9000 ± 2730 MFs m^{-3}); (ii) high densities in the Arctic Ocean, except inside the Beaufort Gyre/Central Arctic ($<2770 \pm 837$ MFs m^{-3}); and (iii) point zones of highest densities inside the Arctic Seas (~$20,000 \pm 19,320$ MFs m^{-3}), such as the east Siberian, Kara, Lapvet, Chukchi, Bering and Beaufort seas; and Hudson Bay (~$27,000 \pm 18,000$ MFs m^{-3}) (Fig. 5).

4. Discussion

Many conclusions regarding the patterns of distribution and accumulation of MPs have been reported for different regions of the marine environment (Lima et al., 2014; Mu et al., 2019; Jiang et al., 2020), as well as for global oceans (Lebreton et al., 2012; Maximenko et al., 2012; van Sebille et al., 2015v; Mountford and Morales Maqueda, 2019). The insights proposed by modelling and simple correlative analyses have concluded that MPs drift in surface or sub-surface waters according to the patterns of ocean currents and accumulate in areas where currents converge, the so-called "ocean gyres" (Jiang et al., 2020; van Sebille
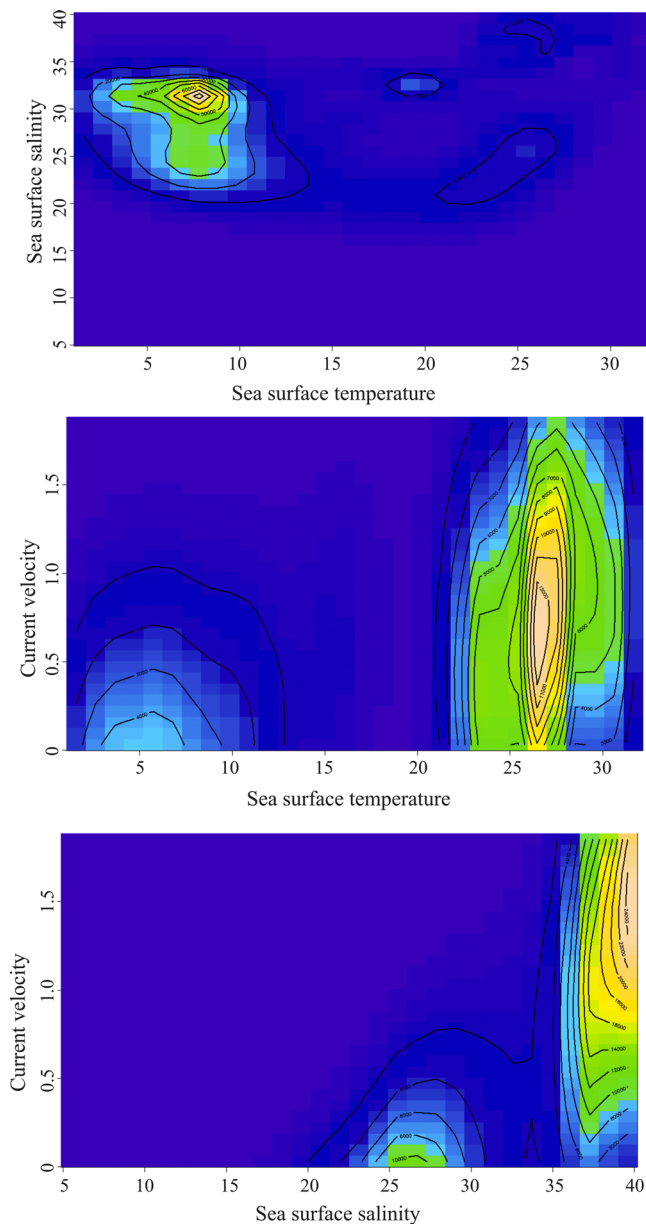
Table 1
Description of environmental satellite parameters. MODIS: Moderate-resolution Imaging Spectroradiometer, WOD: World Ocean Database, ARMOR: Global Observed Ocean Physics Reprocessing (resolution: 0.25°), ORAP: Global Ocean Physics Reanalysis ECMWF (resolution: 0.25°), ECMWF: European Center for Medium Range Weather Forecast (resolution: 0.75°).

Parameter	Abbreviation	Units	Sensor/Model	Resolution	Source of climate data	Sources of reanalyses	References
Sea Surface Temperature	SST	°C	Aqua-MODIS		ARMOR		
Sea Surface Salinity	SSS	PSS	WOD 2009	0.083°		bio-oracle.org	Assis et al., 2017
Current Velocity	CVEL	m s^{-1}	Multiple		ORAP		
Wind Speed	WS	m s^{-1}	Multiple	0.75°	ECMWF	apps.ecmwf.int	Dee et al., 2011

Fig. 2. 2-D interaction plots of the type "response" showing the density of microplastics as predicted by the first smooth term [s(SST, SSS, CVEL)] of the selected model. Unit of MP density: particles m^{-3}.

et al., 2015v). In a global perspective, Lagrangian and Eulerian particle tracking simulations have concluded that the accumulation of MPs are ruled by wind-driven Ekman currents, geostrophyc currents and/or wave-driven stokes drifters (van Sebille et al., 2015v; Mountford and Morales Maqueda, 2019; Onink et al., 2019). On the other hand, correlative models have concluded that temperature, salinity and winds are significant predictors of MP accumulation according to local approaches (Lusher et al., 2015; Kanhai et al., 2017, 2018).

This is the first study attempting to understand the influence of water masses (i.e. large volumes of water where both the temperature and salinity are relatively constant), current velocities and winds in MF accumulation under a global perspective. The model provides global estimates based on an extensive dataset on global ocean grab sampling effort. The outputs of the spatial mapping matches the patterns predicted not only by every global study on MPs to date (van Sebille et al., 2015v; Isobe et al., 2017; Mountford and Morales Maqueda, 2019; Onink et al., 2019), but also by the conclusions of studies reporting

oceanic regional approaches (Cincinelli et al., 2017; Zhu et al., 2018; Jiang et al., 2020). The main objective here is to provide additional information that, together with other global models, will help in the understanding of surface MF distribution. Although this might be a dauting task, coupling the results of the available and future predictive models is the only way to understand the complex relationship among MF buoyancy and sinking capacities and their distribution towards sediments and back to the surface according to physico-chemical dynamics (Hardesty et al., 2017; Cózar et al., 2017; Mountford and Morales Maqueda, 2019; Kane et al., 2020).

From the 300 GAMs, only the models including SST and SSS as predictors had the deviance explained above 10 %. Geostrophic, Ekman and Eulerian currents, drogue drifter trajectories, winds, as well as their northward and eastward components, had low power to explain MF distribution in the absence of SST and SSS (less than 6 % of deviance explained). The final model included the interaction among SST, SSS and CVEL, as well as WS as main effects (31 % of deviance explained). Thus, surface water masses, surface global currents and the influence of near-surface winds have a great role in the patterns of MF distribution and accumulation. According to the relative importance of these variables, MFs are predicted to accumulate in regions of slow cold surface currents and dense surface water-masses. As well, zones of divergences between westerlies and trade winds are predicted to accumulate MFs, which coincides with the location of tropical oceanic gyres. Our model also predicted that MFs accumulate in the Atlantic and Pacific Gyres, Pacific subpolar gyre, Indian Ocean gyre and Mediterranean Sea, which agrees with most observations to date (van Sebille et al., 2015v; Isobe et al., 2017; Mountford and Morales Maqueda, 2019; Onink et al., 2019). Moreover, the model had the sensibility to detect an accumulation pattern of MFs around Antarctica (~6800 ± 2000 MFs m^{-3}), between 50 °S and 60 °S, while close to the Antarctic Coast, MFs presented low density (~2600 ± 1800 MFs m^{-3}). This implies that the Antarctic Circumpolar Current traps MFs and might spread them later towards and beyond the Antarctic Ocean (Isobe et al., 2017; Waller et al., 2017; Lacerda et al., 2019), but coastal accumulation is less probable, possibly due to the sinking of dense waters close to the continent, as observed in the Ross Sea (Cincinelli et al., 2017).

Microfibers, as well, do not accumulate in the Northern Atlantic (~1840 ± 1720 MFs m^{-3}), between 40 °N and 60 °N, where the warm branch of the Thermohaline Circulation currents flow poleward, cool and eventually sink to form the cold North Atlantic Deep Water. This pattern is confirmed by surveys using water pumping in the Eastern Atlantic above 40 °N, where waters southward the Svalbard archipelago (Lusher et al., 2015), surrounding Ireland and United Kingdom (Lusher et al., 2014) and along the coasts of Portugal, Spain and France (Kanhai et al., 2017) presented low densities of MPs (0–22.5 MP s m^{-3}). The model also had sensibility to detect that MFs do not accumulate in major coastal upwelling regions possibly due to the wind-induced Ekman transport offshore, such as observed at the upwelling system of the Ría de Vigo Estuary (Spain). There, floating MPs are flushed out the estuary as ruled by the seaward wind-induced and gravitational circulation (Díez-Minguito et al., 2020).

The highest densities of MFs were predicted to occur in the Arctic Ocean; and it is possibly a response of the North Atlantic and North Pacific currents flowing to the Arctic. Although plastic accumulation at polar latitudes has been overlooked (Cózar et al., 2017), the Arctic sea ice and sediments are acknowledged as temporary sinks for MPs (Peeken et al., 2018; Obbard, 2018; Bergmann et al., 2017). Sea ice can accumulate up to 1.2×10^7 MPs m^{-3} in a single ice core (Peeken et al., 2018; Obbard, 2018), while sediments bellow 2340 m depth accumulate up to 6595 MPs kg^{-1} (Bergmann et al., 2017). However, little is known about the patterns that rule such accumulation. Only recently, it had been reported that the transport of MPs towards the Arctic seas is ruled by wave-driven stokes drifts (Onink et al., 2019). It was also asserted that the Greenland Sea Gyre increases MP pollution in the Nordic Sea [800 to 3740 MPs m^{-3} (method: water pumping)] and that the warm Norwegan
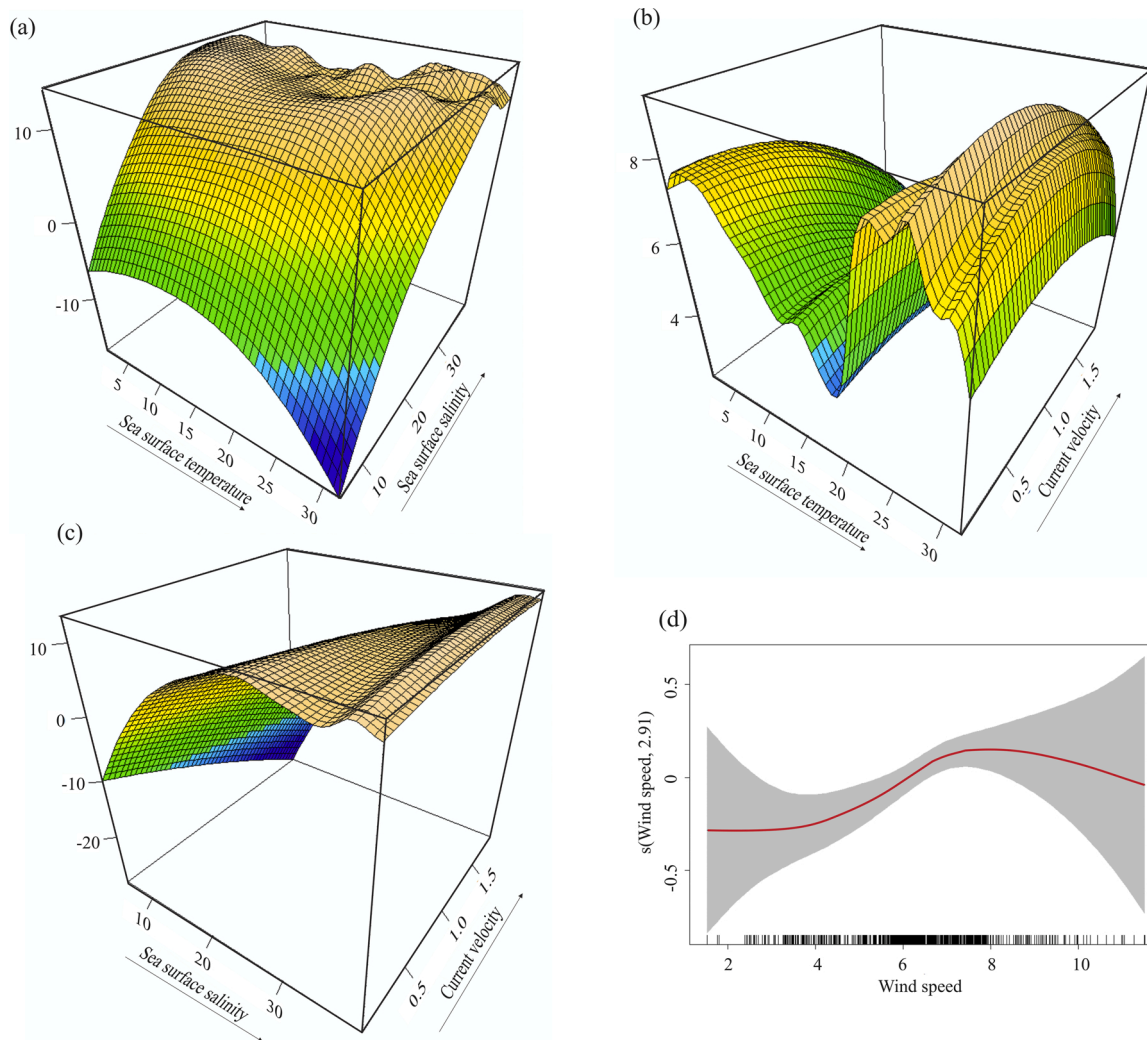
Fig. 3. (a)-(c): 3-D interaction plots. The *x* and *y*-axis of the interaction plots reflect the relative importance of each variable in the model and the interaction effect is presented on the *z*-axis. (d): Single variable effect plot for the second smooth term [s(WS)]. The dashes on the *x*-axis, the so-called 'rug', indicate the density of points for the different variable values. The solid red line indicates the GAM coefficients, and the shadowed grey area represents the 95 % point-wise confidence bands at $p = 0.05$. GAM: MP ~ s(SST, SSS, CVEL) + s(WS).
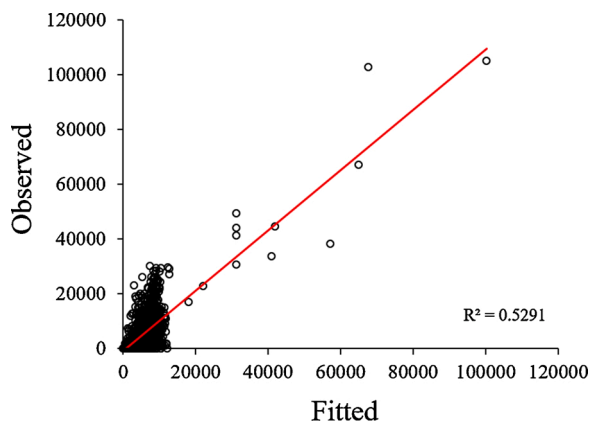

Fig. 4. Scatter plot for the relationship between the observed and the fitted density of microfibers (items m^{-3}).

current is likely to flush MPs from the Gyre to the Arctic Ocean (Jiang et al., 2020). This emphasizes the finding of Morgana et al. (2018), who found high number of fibers, ranging from 4×10^4 to 6×10^5 MPs m^{-3} (method: water pumping) in the Northeast Greenland. Moreover, the

North Atlantic branch of the Thermohaline Circulation is possibly transferring floating debris from the North Atlantic to the Arctic seas (Cózar et al., 2017).

Similarly, our results predicted that the Gulf stream, the North Atlantic and the Norwegian currents are flushing MFs from the North Atlantic Gyre towards the Arctic Ocean following eastern Greenland, the Svalbard Archipelago and the north coast of Russia. As well, MPs from the North Pacific Gyre and from the subpolar Pacific gyre are being flushed towards the Arctic through the Bering Strait by the Alaska Coastal Current. Once in the Arctic, it is reasonable to conclude that the accumulation of MF occurs outside the Beaufort gyre (2800 ± 840 MFs m^{-3}), since it is a zone of accumulation of sea ice and freshwater and, thus, MPs are predicted to peak in the east Siberian, Chukchi, Bering, Beaufort seas and Hudson Bay [~$20,000 \pm 19,320$ MFs m^{-3} (Range: ~2420 to ~92,000 MFs m^{-3})]. Finally, MFs are transported back to the North Atlantic by the Labrador current. This agrees with recent studies, which have concluded that the Arctic Sea might be a dead end for floating MPs (Cózar et al., 2017; Onink et al., 2019; Jiang et al., 2020).

The Lagrangian simulation proposed by Onink et al. (2019) concluded that geostrophic currents and stokes drift do not contribute to MP accumulation. Rather, total currents had a greater power in MP accumulation not only in subtropical gyres, but also in the Arctic Ocean, corroborating the global models proposed by Cózar et al. (2014, 2017),

Table 3
Density of microfilaments in different oceanic regions as predicted by the GAM model: MP ~ s(SST, SSS, CVEL) + s(WS).

Oceanic region	Min	Max	mean
Global Ocean	0	113160	5900 ± 6800
Arctic Ocean			
Arctic Central	1000	6400	2770 ± 837
Arctic Seas	2420	91650	20000 ± 19320
Hudson Bay	1500	99000	27390 ± 18500
Barents Sea	1800	13200	5400 ± 2430
Atlantic Ocean			
Northeast Greenland	1360	28750	7640 ± 7000
South Svalbard	1740	8630	4600 ± 1800
Northern Atlantic (40 °N-60 °N)	300	7770	1800 ± 1720
Northeast Atlantic (Portugal, Spain and France)	320	11500	2720 ± 2600
Baltic Sea	0	19400	1760 ± 4500
North Atlantic Gyre	845	16000	8450 ± 2600
South Atlantic Gyre	490	11700	5800 ± 2470
Equatorial Atlantic	1736	11450	4500 ± 1600
Mediterranean	870	15800	8700 ± 2700
Black Sea	290	2000	930 ± 460
Pacifi Ocean			
Northeast Pacific	2350	20270	7000 ± 4200
North Pacific Gyre	2360	20400	7450 ± 3240
South Pacific Gyre	660	12620	1600 ± 3000
Equatorial Pacific	1270	8000	3200 ± 1600
Red Sea	311	4230	1770 ± 1190
Persian Gulf	40	2000	500 ± 630
Sea of Japan	760	19000	5450 ± 3600
Sea of Okhotsk	1793	7968	5000 ± 1440
Idian Ocean			
Bay of Bengal	1520	5160	3800 ± 800
Indian Central	1562	10646	3000 ± 1270
Indian Gyre	450	7000	3000 ± 2190
Antarctic Ocean			
Antarctic Circumpolar Current (55 °S-65 °S)	1120	12200	6800 ± 2000
Antartica Coast	626	8823	2600 ± 1800
Ross Sea	1100	5500	2700 ± 950

Eriksen et al. (2014); Onink et al. (2019) and ours. However, accurate comparative approaches between our model and the available ones are not possible due to different sampling methods and because, at least to the available models for floating MPs, their accumulation in Polar Oceans is misunderstood due to the absence of accurate data on ocean currents and drifters above 70 °N and bellow 70 °S (Lebreton et al., 2012; Maximenko et al., 2012; van Sebille et al., 2015v; Onink et al., 2019).

The predictions of our study are in agreement with recent publications concerning the underestimation of floating MPs by plankton nets, since their small size and flexibility might push them out of the net during a tow (Barrows et al., 2018; Conkle et al., 2018). Between 50 % and 90 % of the floating MPs sampled in the marine environment, regardless sampling methods, are MFs. However, oceanic studies reporting sampling with 1 L grab are scarce and few have used continuous intake water pumping (Desforges et al., 2014; Zhu et al., 2018; Jiang et al., 2020). So, this is still difficult to make an accurate comparison of quantities between these two methods, especially regarding sampling design. These methods can collect densities of MPs several orders of magnitude higher than those collected with plankton nets. 1 L grab sampling have been recently acknowledged as an accepted method for collecting microplastics due to the ability to capture plastic at the micro- and nano-size, often not precisely accounted in plankton tows (Barrows at al., 2017, 2018). On the other hand, the small sample volume seems to be a limitation because grab do not allow the coverage of a larger area and may result in high variability among samples collected far from each other.

Regarding MFs, here it was noted that the average amount collected and estimated by our study using 1 L grab (6208 and 5900 MFs m^{-3}, respectively) have a similar or comparable order of magnitude when compared to studies using water pumping. The variations in quantification are likely related to the spatio-temporal variability in sampling designs. For example, in the Greenland Sea, MPs collected with plankton net had a maximum density of 4.52 MPs m^{-3} (Amélineau et al., 2016), but this density increased up to 2430 MPs m^{-3} in the Greenland sea gyre (Jiang et al., 2020) and up to 6×10^5 MPs m^{-3} in Northeast Greenland (Morgana et al., 2018) when collected by water pumping. In the northwestern Pacific, MPs collected with plankton net peaked to a maximum of 0.035 MPs m^{-3} (Mu et al., 2019), while in the northeastern Pacific it was up to 9181 MPs m^{-3} with water pumping (Desforges et al., 2014). As well, in the Yellow sea (China), MPs collected with plankton net peaked to a maximum of 0.81 MPs m^{-3} (Sun et al., 2018), and increased up to 1000 MPs m^{-3} when collected by water pumping (Zhu et al., 2018). Even the highest value predicted in the van Sebille model (10 MPs m^{-3}), which used plankton nets, is three orders of magnitude lower than the average predicted by our model (*i.e.* 5900 ± 6800 MFs m^{-3}) (van Sebille et al., 2015). Most of these studies asserted that >75 %
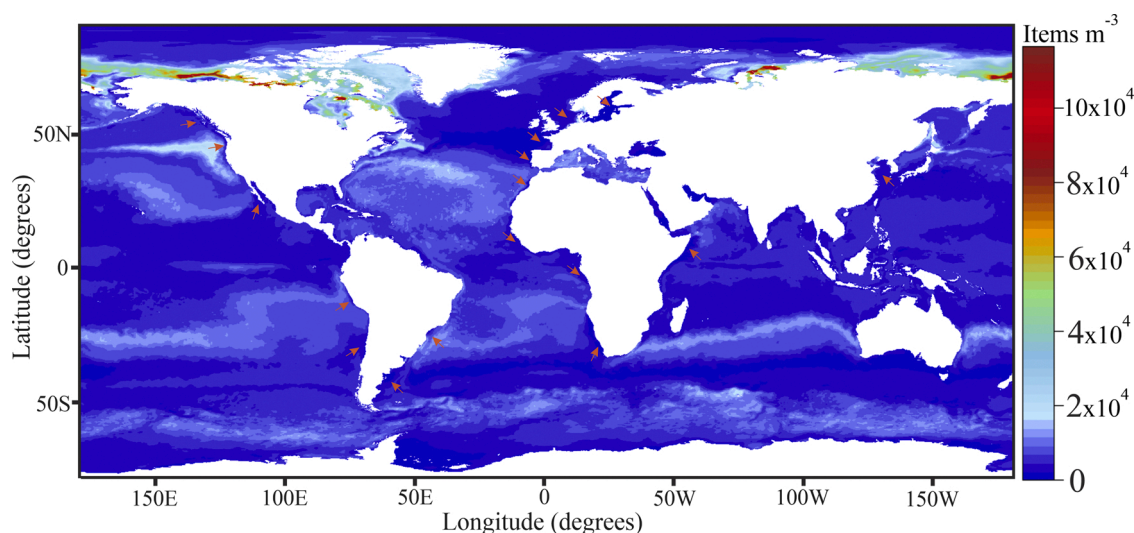

Fig. 5. Map of spatial distribution indicating the variability in microplastic density (particles m^{-3}) as predicted by the selected model: MP ~ s(SST, SSS, CVEL) + s (WS). Arrows indicate the major coastal upwelling systems. Geographic coordinate system: WGS 1984.

of the MPs found in samples are MFs. Therefore, it seems that the quantification of MFs collected with 1 L grab is not too different of the amount available in the surrounding 1000 L (or 1 m^{-3}).

In 2016, 9 million tons of fibers were produced globally, divided as nearly 60 % synthetic fibers and 40 % natural fibers (Barrows et al., 2018). Polyester represents the greatest share of microfiber pollution and its sale accounts for half of the global fiber market (Carr, 2017). Whereas it is estimated that $\sim$ 2.5 million tons of microfibers are released into the ocean every year *via* river input (Boucher and Friot, 2017; Mishra et al., 2019), it is not difficult to conclude that we have been underestimating microfibers until recently. It is now acknowledged that the current density of microplastics in the ocean is 3 orders of magnitude higher than previously asserted (Barrows et al., 2018). Although many studies have transformed volume into area to increase robustness during modelling and to visually rise the amount of MPs, this does not mean that every study to date has inappropriate conclusions regarding the fate of microplastics in the marine environment (Lima et al., 2014; van Sebille et al., 2015v; Onink et al., 2019). Rather, environmental pollution assessments urge new methodological procedures to confirm what is really going on in the global oceans. Fibers are even a special case, since they have been reported as commonly ingested by the marine fauna and their toxicity capacity is still not properly understood (Remy et al., 2015; Zhao et al., 2016; Ferreira et al., 2019).

Despite rivers being the main exporters of MPs towards the ocean (Lima et al., 2014; Lebreton et al., 2017), it was predicted that coastal areas have low potential for accumulation, and this is also true for upwelling systems. Instead, MFs are being flushed offshore to oceanic gyres and from the gyres towards the poles, far from pollution sources (Bergmann et al., 2017; Cózar et al., 2017; Law et al., 2014). In addition, the warm branch of the Thermohaline Circulation is likely to have a great role in the transport of MFs, emphasizing that surface water masses are important predictors. Such warmer flow has the potential to carry floating MFs of the entire ocean basin; and once it reaches the Northern Atlantic and Northern Pacific Oceans, the MFs are flushed towards the Arctic Ocean, where several point zones of accumulation are observed.

CRediT authorship contribution statement

André R.A. Lima: Conceptualization, Funding acquisition, Investigation, Methodology, Validation, Visualization, Writing - original draft. **Guilherme V.B. Ferreira:** Conceptualization, Funding acquisition, Investigation, Methodology, Validation, Visualization, Writing - original draft. **Abigail P.W. Barrows:** Conceptualization, Funding acquisition, Investigation, Methodology, Data curation, Project administration, Resources. **Katie S. Christiansen:** Conceptualization, Funding acquisition, Investigation, Methodology, Data curation, Project administration, Resources, Writing - review & editing. **Gregg Treinish:** Conceptualization, Funding acquisition, Investigation, Methodology, Data curation, Project administration, Resources. **Michelle C. Toshack:** Conceptualization, Funding acquisition, Investigation, Methodology, Data curation, Project administration, Resources.

Declaration of Competing Interest

The authors declare that they have no known competing financial interests or personal relationships that could have appeared to influence the work reported in this paper.

Appendix A. Supplementary data

Supplementary material related to this article can be found, in the online version, at doi:https://doi.org/10.1016/j.jhazmat.2020.123796.

References

Amélineau, F., Bonnet, D., Heitz, O., Mortreux, V., Harding, A.M.A., Karnovsky, N., Walkusz, W., Fort, J., Grémillet, D., 2016. Microplastic pollution in the Greenland Sea: background levels and selective contamination of planktivorous diving seabirds. Environ. Pollut. 219, 1131–1139. https://doi.org/10.1016/j.envpol.2016.09.017.

Assis, J., Tyberghein, L., Bosch, S., Verbruggen, H., Serrão, E.A., De Clerck, O., 2017. Bio-ORACLE v2.0: extending marine data layers for bioclimatic modelling. Glob. Ecol. Biogeogr. 27, 277–284. https://doi.org/10.1111/geb.12693.

Barrows, A.P.W., Neumann, C.A., Berger, M.L., Shaw, S.D., 2017. Grab vs. Neuston tow net: a microplastic sampling performance comparison and possible advances in the field. Anal. Methods 9, 1446–1453. https://doi.org/10.1039/C6AY02387H.

Barrows, A.P.W., Cathey, S.E., Petersen, C.W., 2018. Marine environment microfiber contamination: Global patterns and the diversity of microparticle origins. Environ. Pollut. 237, 275–284. https://doi.org/10.1016/j.envpol.2018.02.062.

Bergmann, M., Wirzberger, V., Krumpen, T., Lorenz, C., Primpke, S., Tekman, M.B., Gerdts, G., 2017. High quantities of microplastic in arctic deep-sea sediments from the HAUSGARTEN observatory. Environ. Sci. Technol. 51, 11000–11010. https://doi.org/10.1021/acs.est.7b03331.

Boucher, J., Friot, D., 2017. Primary Microplastics in the Oceans: a Global Evaluation of Sources. IUCN, Gland, Switzerland. https://doi.org/10.2305/IUCN.CH.2017.0.

Carr, S.A., 2017. Sources and dispersive modes of micro-fibers in the environment. Integr. Environ. Assess. Manag. 13, 466–469. https://doi.org/10.1002/ieam.1916.

Cincinelli, A., Scopetani, C., Chelazzi, D., Lombardini, E., Martellini, T., Katsoyiannis, A., Fossi, M.C., Corsolini, S., 2017. Microplastic in the surface waters of the Ross Sea (Antarctica): occurrence, distribution and characterization by FTIR. Chemosphere 175, 391–400. https://doi.org/10.1016/j.chemosphere.2017.02.024.

Conkle, J.L., Báez Del Valle, C.D., Turner, J.W., 2018. Are we underestimating microplastic contamination in aquatic environments? Environ. Manage. 61, 1–8. https://doi.org/10.1007/s00267-017-0947-8.

Cozar, A., Echevarria, F., Gonzalez-Gordillo, J.I., Irigoien, X., Ubeda, B., Hernandez-Leon, S., Palma, A.T., Navarro, S., Garcia-de-Lomas, J., Ruiz, A., Fernandez-de-Puelles, M.L., Duarte, C.M., 2014. Plastic debris in the open ocean. Proc. Natl. Acad. Sci. 111, 10239–10244. https://doi.org/10.1073/pnas.1314705111.

Cózar, A., Martí, E., Duarte, C.M., García-de-Lomas, J., Van Sebille, E., Ballatore, T.J., Eguíluz, V.M., Ignacio González-Gordillo, J., Pedrotti, M.L., Echevarría, F., Troublè, R., Irigoien, X., 2017. The Arctic Ocean as a dead end for floating plastics in the North Atlantic branch of the Thermohaline Circulation. Sci. Adv. 3, 1–9. https://doi.org/10.1126/sciadv.1600582.

Dauvergne, P., 2018. Why is the global governance of plastic failing the oceans? Glob. Environ. Chang. 51, 22–31. https://doi.org/10.1016/j.gloenvcha.2018.05.002.

Dee, D.P., Uppala, S.M., Simmons, A.J., Berrisford, P., Poli, P., Kobayashi, S., Andrae, U., Balmaseda, M.A., Balsamo, G., Bauer, P., Bechtold, P., Beljaars, A.C.M., van de Berg, L., Bidlot, J., Bormann, N., Delsol, C., Dragani, R., Fuentes, M., Geer, A.J., Haimberger, L., Healy, S.B., Hersbach, H., Hólm, E.V., Isaksen, L., Kållberg, P., Köhler, M., Matricardi, M., Mcnally, A.P., Monge-Sanz, B.M., Morcrette, J.J., Park, B. K., Peubey, C., de Rosnay, P., Tavolato, C., Thépaut, J.N., Vitart, F., 2011. The ERA-Interim reanalysis: configuration and performance of the data assimilation system. Q. J. R. Meteorol. Soc. 137, 553–597. https://doi.org/10.1002/qj.828.

Desforges, J.P.W., Galbraith, M., Dangerfield, N., Ross, P.S., 2014. Widespread distribution of microplastics in subsurface seawater in the NE Pacific Ocean. Mar. Pollut. Bull. 79, 94–99. https://doi.org/10.1016/j.marpolbul.2013.12.035.

Díez-Minguito, M., Bermúdez, M., Gago, J., Carretero, O., Viñas, L., 2020. Observations and idealized modelling of microplastic transport in estuaries: The exemplary case of an upwelling system (Ría de Vigo, NW Spain). Mar. Chem. 222, 103780 https://doi.org/10.1016/j.marchem.2020.103780.

Enfrin, M., Lee, J., Gibert, Y., Basheer, F., Kong, L., Dumée, L.F., 2020. Release of hazardous nanoplastic contaminants due to microplastics fragmentation under shear stress forces. J. Hazard. Mater. 384, 121393 https://doi.org/10.1016/j.jhazmat.2019.121393.

Eriksen, M., Lebreton, L.C.M., Carson, H.S., Thiel, M., Moore, C.J., Borerro, J.C., Galgani, F., Ryan, P.G., Reisser, J., 2014. Plastic Pollution in the World's Oceans: More than 5 Trillion Plastic Pieces Weighing over 250,000 Tons Afloat at Sea. PLoS One 9. https://doi.org/10.1371/journal.pone.0111913.

Eriksen, M., Thiel, M., Prindiville, M., Kiessling, T., 2018. Microplastic: what are the solutions?. In: Wagner, M., Lambert, S. (Eds.), Freshwater Microplastics. The Handbook of Environmental Chemistry, vol 58. Springer, Cham. https://doi.org/10.1007/978-3-319-61615-5_13.

ESR, 2009. OSCAR Third Degree Resolution Ocean Surface Currents [WWW Document]. Ver. 1. PO.DAAC, CA, USA. https://doi.org/10.5067/OSCAR-03D01.

Ferreira, G.V.B., Barletta, M., Lima, A.R.A., Morley, S.A., Costa, M.F., 2019. Dynamics of marine debris ingestion by profitable fishes along the estuarine ecocline. Sci. Rep. 9, 13514. https://doi.org/10.1038/s41598-019-49992-3.

Gatidou, G., Arvaniti, O.S., Stasinakis, A.S., 2019. Review on the occurrence and fate of microplastics in Sewage Treatment Plants. J. Hazard. Mater. 367, 504–512. https://doi.org/10.1016/j.jhazmat.2018.12.081.

Hardesty, B.D., Harari, J., Isobe, A., Lebreton, L., Maximenko, N., Potemra, J., van Sebille, E., Dick Vethaak, A., Wilcox, C., 2017. Using numerical model simulations to improve the understanding of micro-plastic distribution and pathways in the marine environment. Front. Mar. Sci. 4, 1–9. https://doi.org/10.3389/fmars.2017.00030.

Hastie, T.J., Tibshirani, R.J., 1990. Generalized Additive Models, 1st ed. Chapman and Hall, London.

Herrera, A., Raymond, E., Martínez, I., Álvarez, S., Canning-Clode, J., Gestoso, I., Pham, C.K., Ríos, N., Rodríguez, Y., Gómez, M., 2019. First evaluation of neustonic microplastics in the Macaronesian region, NE Atlantic. Mar. Pollut. Bull. 153, 110999 https://doi.org/10.1016/j.marpolbul.2020.110999.

Hijmans, R.J., van Etten, J., Sumner, M., Cheng, J., Bevan, A., Bivand, R., Busetto, L., Canty, M., Forrest, D., Ghosh, A., Golicher, D., Gray, J., Greenberg, J.A., Hiemstra, P., Hingee, K., Karney, C., Mattiuzzi, M., Mosher, S., Nowosad, J., Pebesma, E., Lamigueiro, O.P., Racine, E.B., Rowlingson, B., Shortridge, A., Venables, B., Wueest, R., 2020. Package 'raster': Geographic Data Analysis and Modeling. Repository CRAN.

Isobe, A., Uchiyama-Matsumoto, K., Uchida, K., Tokai, T., 2017. Microplastics in the Southern Ocean. Mar. Pollut. Bull. 114, 623–626. https://doi.org/10.1016/j.marpolbul.2016.09.037.

Jiang, Y., Yang, F., Zhao, Y., Wang, J., 2020. Greenland Sea Gyre increases microplastic pollution in the surface waters of the Nordic Seas. Sci. Total Environ. 712, 136484 https://doi.org/10.1016/j.scitotenv.2019.136484.

Kane, I.A., Clare, M.A., Miramontes, E., Wogelius, R., Rothwell, J.J., Garreau, P., Pohl, F., 2020. Seafloor microplastic hotspots controlled by deep-sea circulation. Science 5899 (80-), 1–8. https://doi.org/10.1126/science.aba5899.

Kanhai, L.D.K., Officer, R., Lyashevska, O., Thompson, R.C., O'Connor, I., 2017. Microplastic abundance, distribution and composition along a latitudinal gradient in the Atlantic Ocean. Mar. Pollut. Bull. 115, 307–314. https://doi.org/10.1016/j.marpolbul.2016.12.025.

Kanhai, L.D.K., Gårdfeldt, K., Lyashevska, O., Hassellöv, M., Thompson, R.C., O'Connor, I., 2018. Microplastics in sub-surface waters of the Arctic Central Basin. Mar. Pollut. Bull. 130, 8–18. https://doi.org/10.1016/j.marpolbul.2018.03.011.

Lacerda, A.L.D.F., Rodrigues, L., dos S., van Sebille, E., Rodrigues, F.L., Ribeiro, L., Secchi, E.R., Kessler, F., Proietti, M.C., 2019. Plastics in sea surface waters around the Antarctic Peninsula. Sci. Rep. 9, 1–12. https://doi.org/10.1038/s41598-019-40311-4.

Laurindo, L.C., Mariano, A.J., Lumpkin, R., 2017. An improved near-surface velocity climatology for the global ocean from drifter observations. Deep. Res. Part I Oceanogr. Res. Pap. 124, 73–92. https://doi.org/10.1016/j.dsr.2017.04.009.

Law, K.L., Morét-Ferguson, S.E., Goodwin, D.S., Zettler, E.R., DeForce, E., Kukulka, T., Proskurowski, G., 2014. Distribution of surface plastic debris in the Eastern Pacific Ocean from an 11-Year data set. Environ. Sci. Technol. 48, 4732–4738. https://doi.org/10.1021/es4053076.

Lebreton, L.C.M., Greer, S.D., Borrero, J.C., 2012. Numerical modelling of floating debris in the world's oceans. Mar. Pollut. Bull. 64, 653–661. https://doi.org/10.1016/j.marpolbul.2011.10.027.

Lebreton, L.C.M., van der Zwet, J., Damsteeg, J.-W., Slat, B., Andrady, A.L., Reisser, J., 2017. River plastic emissions to the world's oceans. Nat. Commun. 8, 15611. https://doi.org/10.1038/ncomms15611.

Li, Y., Lu, Z., Zheng, H., Wang, J., Chen, C., 2020. Microplastics in surface water and sediments of Chongming Island in the Yangtze Estuary, China. Environ. Sci. Eur. 32 https://doi.org/10.1186/s12302-020-0297-7.

Lima, A.R.A., Costa, M.F., Barletta, M., 2014. Distribution patterns of microplastics within the plankton of a tropical estuary. Environ. Res. 132, 146–155. https://doi.org/10.1016/j.envres.2014.03.031.

Lima, A.R.A., Silva, M.D., Possatto, F.E., Ferreira, G.V.B., Krelling, A.P., 2020. Plastic contamination in Brazilian Freshwater and coastal environments: a source-to-Sea transboundary approach. Handbook of Environmental Chemistry, pp. 1–12. https://doi.org/10.1007/698_2020_514.

Lusher, A.L., Burke, A., O'Connor, I., Officer, R., 2014. Microplastic pollution in the Northeast Atlantic Ocean: validated and opportunistic sampling. Mar. Pollut. Bull. 88, 325–333. https://doi.org/10.1016/j.marpolbul.2014.08.023.

Lusher, A.L., Tirelli, V., O'Connor, I., Officer, R., 2015. Microplastics in Arctic polar waters: the first reported values of particles in surface and sub-surface samples. Sci. Rep. 5, 1–9. https://doi.org/10.1038/srep14947.

Marra, G., Wood, S.N., 2011. Practical variable selection for generalized additive models. Comput. Stat. Data Anal. 55, 2372–2387. https://doi.org/10.1016/j.csda.2011.02.004.

Maximenko, N., Hafner, J., Niiler, P., 2012. Pathways of marine debris derived from trajectories of Lagrangian drifters. Mar. Pollut. Bull. 65, 51–62. https://doi.org/10.1016/j.marpolbul.2011.04.016.

Mertz, F., Legeais, J.-F., 2019. Copernicus Climate Change Service. Product User Guide and Specification. Sea Level v1.1 [WWW Document]. URL https://cds.climate.copernicus.eu/cdsapp#!/dataset/satellite-sea-level-global?tab=overview. (last access: 04 April 2020).

Mishra, S., Rath, Ccharan, Das, A.P., 2019. Marine microfiber pollution: a review on present status and future challenges. Mar. Pollut. Bull. 140, 188–197. https://doi.org/10.1016/j.marpolbul.2019.01.039.

Morgana, S., Ghigliotti, L., Estévez-Calvar, N., Stifanese, R., Wieckzorek, A., Doyle, T., Christiansen, J.S., Faimali, M., Garaventa, F., 2018. Microplastics in the Arctic: a case study with sub-surface water and fish samples off Northeast Greenland. Environ. Pollut. 242, 1078–1086. https://doi.org/10.1016/j.envpol.2018.08.001.

Mountford, A.S., Morales Maqueda, M.A., 2019. Eulerian modeling of the three-dimensional distribution of seven popular microplastic types in the Global Ocean. J. Geophys. Res. Ocean 124, 8558–8573. https://doi.org/10.1029/2019JC015050.

Mu, J., Zhang, S., Qu, L., Jin, F., Fang, C., Ma, X., Zhang, W., Wang, J., 2019. Microplastics abundance and characteristics in surface waters from the Northwest Pacific, the Bering Sea, and the Chukchi Sea. Mar. Pollut. Bull. 143, 58–65. https://doi.org/10.1016/j.marpolbul.2019.04.023.

Mulet, S., Rio, M.-H., Mignot, A., Guinehut, S., Morrow, R., 2012. A new estimate of the global 3D geostrophic ocean circulation based on satellite data and in-situ measurements. Deep Sea Res. Part II Top. Stud. Oceanogr. 77–80, 70–81. https://doi.org/10.1016/j.dsr2.2012.04.012.

Niaounakis, M., 2017. Regulatory framework. in: Management of Marine Plastic Debris. 361–413.

Obbard, R.W., 2018. Microplastics in Polar Regions: the role of long range transport. Curr. Opin. Environ. Sci. Heal. 1, 24–29. https://doi.org/10.1016/j.coesh.2017.10.004.

Onink, V., Wichmann, D., Delandmeter, P., van Sebille, E., 2019. The role of ekman currents, geostrophy, and stokes drift in the accumulation of floating microplastic. J. Geophys. Res. Ocean 124, 1474–1490. https://doi.org/10.1029/2018JC014547.

Peeken, I., Primpke, S., Beyer, B., Gütermann, J., Katlein, C., Krumpen, T., Bergmann, M., Hehemann, L., Gerdts, G., 2018. Arctic sea ice is an important temporal sink and means of transport for microplastic. Nat. Commun. 9 https://doi.org/10.1038/s41467-018-03825-5.

R Core Team, 2020. R: a language and environment for statistical computing. R Foundation for Statistical Computing.

Rascle, N., Ardhuin, F., 2013. A global wave parameter database for geophysical applications. Part 2: Model validation with improved source term parameterization. Ocean Model 70, 174–188. https://doi.org/10.1016/j.ocemod.2012.12.001.

Raubenheimer, K., McIlgorm, A., 2018. Can the Basel and Stockholm Conventions provide a global framework to reduce the impact of marine plastic litter? Mar. Policy 96, 285–290. https://doi.org/10.1016/j.marpol.2018.01.013.

Remy, F., Collard, F., Gilbert, B., Compère, P., Eppe, G., Lepoint, G., 2015. When microplastic is not plastic: the ingestion of artificial cellulose fibers by macrofauna living in seagrass macrophytodetritus. Environ. Sci. Technol. 49, 11158–11166. https://doi.org/10.1021/acs.est.5b02005.

Rio, M.-H., Mulet, S., Picot, N., 2014. Beyond GOCE for the ocean circulation estimate: synergetic use of altimetry, gravimetry, and in situ data provides new insight into geostrophic and Ekman currents. Geophys. Res. Lett. 41, 8918–8925. https://doi.org/10.1002/2014GL061773.

Sun, X., Liang, J., Zhu, M., Zhao, Y., Zhang, B., 2018. Microplastics in seawater and zooplankton from the Yellow Sea. Environ. Pollut. 242, 585–595. https://doi.org/10.1016/j.envpol.2018.07.014.

Tweedie, M.C.K., 1984. An index which distinguishes between some important exponential families. In: Ghosh, J.K., Roy, J. (Eds.), Statistics: Applications and New Directions. Indian Statistical Institute, Calcutta, pp. 579–604. Proceedings of the Indian Statistical Institute Golden Jubilee International Conference.

van Sebille, E., Wilcox, C., Lebreton, L., Maximenko, N., Hardesty, B.D., Van Franeker, J. A., Eriksen, M., Siegel, D., Galgani, F., Law, K.L., 2015v. A global inventory of small floating plastic debris. Environ. Res. Lett. 10 https://doi.org/10.1088/1748-9326/10/12/124006.

Waller, C.L., Griffiths, H.J., Waluda, C.M., Thorpe, S.E., Loaiza, I., Moreno, B., Pacherres, C.O., Hughes, K.A., 2017. Microplastics in the Antarctic marine system: an emerging area of research. Sci. Total Environ. 598, 220–227. https://doi.org/10.1016/j.scitotenv.2017.03.283.

Wood, S.N., 2006. Generalized Additive Models: An Introduction with R, 1st ed. Chapman and Hall/CRC, Boca Raton, Florida, USA.

Wood, S.N., 2019. Package 'mgcv': Mixed GAM Computation Vehicle with Automatic Smoothness Estimation. Repository CRAN.

Woodall, L.C., Sanchez-Vidal, A., Canals, M., Paterson, G.L.J., Coppock, R., Sleight, V., Calafat, A., Rogers, A.D., Narayanaswamy, B.E., Thompson, R.C., 2014. The deep sea is a major sink for microplastic debris. R. Soc. Open Sci. 1, 140317 https://doi.org/10.1098/rsos.140317.

Wu, N., Zhang, Y., Zhang, X., Zhao, Z., He, J., Li, W., Ma, Y., Niu, Z., 2019. Occurrence and distribution of microplastics in the surface water and sediment of two typical estuaries in Bohai Bay, China. Environ. Sci. Process. Impacts 21, 1143–1152. https://doi.org/10.1039/c9em00148d.

Yang, H., Xiong, H., Mi, K., Xue, W., Wei, W., Zhang, Y., 2020. Toxicity comparison of nano-sized and micron-sized microplastics to Goldfish *Carassius auratus* Larvae. J. Hazard. Mater. 388, 122058 https://doi.org/10.1016/j.jhazmat.2020.122058.

Yu, F., Yang, C., Zhu, Z., Bai, X., Ma, J., 2019. Adsorption behavior of organic pollutants and metals on micro/nanoplastics in the aquatic environment. Sci. Total Environ. 694, 133643 https://doi.org/10.1016/j.scitotenv.2019.133643.

Zettler, E.R., Takada, H., Monteleone, B., Mallos, N., Eriksen, M., Amaral-Zettler, L.A., 2017. Incorporating citizen science to study plastics in the environment. Anal. Methods 9, 1392–1403. https://doi.org/10.1039/C6AY02716D.

Zhao, S., Zhu, L., Li, D., 2016. Microscopic anthropogenic litter in terrestrial birds from Shanghai, China: not only plastics but also natural fibers. Sci. Total Environ. 550, 1110–1115. https://doi.org/10.1016/j.scitotenv.2016.01.112.

Zhu, L., Bai, H., Chen, B., Sun, X., Qu, K., Xia, B., 2018. Microplastic pollution in North Yellow Sea, China: observations on occurrence, distribution and identification. Sci. Total Environ. 636, 20–29. https://doi.org/10.1016/j.scitotenv.2018.04.182.

Electronic references

European Commission, 2018. A European Strategy for Plastics in a Circular Economy. Communication from the Commission to the European Parliament, the Council, the European Economic and Social Committee and the Committee of the Regions. Available from: https://ec.europa.eu/environment/circular-economy/pdf/plastics-strategy-brochure.pdf.

U.S. Congress, 2015. Microbead-Free Waters of 2015. 114th Congress Public Law 114. House of Energy and Commerce. Available from: https://www.congress.gov/bill/114th-congress/house-bill/1321/text